CellPress

The Beauty of a Visualized Peroxo-diiron(III) Intermediate

Gerhard Grüber[1,*]
[1]School of Biological Sciences, Nanyang Technological University, 60 Nanyang Drive, Singapore 637551, Republic of Singapore
*Correspondence: grueber@ntu.edu.sg
http://dx.doi.org/10.1016/j.str.2015.04.010

Deoxyhypusine synthase (DHS) and deoxyhypusine hydroxylase (DOHH) are essential for hypusination of eukaryotic translation initiation factor 5A (eIF-5A). In this issue, Han et al. use X-ray crystallograpy and UV/Vis and Mössbauer spectroscopy to provide insights into the fundamental mechanism of the hypusination of eIF-5A and a peroxo intermediate state.

The non-heme diiron enzymes catalyzing the oxidation of hydrocarbons became the focus of industrial applications, like the soluble methane monooxygenase hydroxylase (sMMOH) from methanotrophic bacteria, which oxidizes methane to methanol (Tinberg and Lippard, 2011). The first step of its reaction cycle (Figure 1) is the interaction of the reduced (Fe(II)-Fe(II)) form of the enzyme with dioxygen to yield a peroxo-diiron(III) species named **P**. This intermediate is subsequently converted into a species termed **Q**, which contains an Fe(IV)-Fe(IV) core (Wallar and Lipscomb, 1996), and is believed to perform the oxidation of methane.

The intermediates **P** and **Q** are only short-lived. A few weeks ago, time-resolved Resonance Raman spectroscopy confirmed the $Fe_2(\mu\text{-}O)_2$ diamond structure of **Q** (Banerjee et al., 2015). The data showed that both μ-oxygen atoms of **Q** are derived from O_2, and suggested homolytic O-O bond cleavage via intermediates such as (I) on the **P**→**Q** path (Figure 1), but not the heterolytic mechanisms (II and III) that require the protonation of the peroxo ligand (Solomon et al., 2000; Xue et al., 2008).

For the structure of the peroxo-diiron(III) intermediate **P**, which precedes **Q**, various configurations have been reviewed. These include μ-1,2 (η^1,η^1-1,2; either *cis* [I in Figure 2A] or *trans* [II in Figure 2A]), an η^2,η^2-1,2 (III in Figure 2A), and a μ-1,1 (η^1,η^1-1,1; IV in Figure 2A) arrangement of the peroxo ligand (Tinberg and Lippard, 2011). Like **Q**, the **P** intermediate of sMMOH is very short-lived ($t_{1/2}$ of about 1.5 s at 4°C) (Liu et al., 1995), making spectroscopic work difficult.

Importantly, there is a human non-heme diiron oxygenase called deoxyhypusine hydroxylase (hDOHH) in which the peroxo-diiron(III) intermediate is stable. Previous Resonance Raman studies of this intermediate suggested a μ-1,2 interaction of the peroxide ion with the diiron core (Vu et al., 2009). In this issue of *Structure*, Han et al. (2015) now present two crystal structures of hDOHH, one of the peroxo-diiron(III) intermediates, and the other of a complex with glycerol. Through time-dependent UV/Vis spectra of the intermediate, which is colored blue (absorption maximum at ~630 nm), they show that the peroxo species, which they have crystallized, does not correspond to the one formed immediately after the reaction of the reduced form of hDOHH with O_2, but to a slightly different one obtained over the time of crystallization (48 hr). This is supported by Mössbauer spectra of the ^{57}Fe-hDOHH in the crystals, which differ slightly from those obtained from freshly prepared hDOHH in solution. In any case, Han et al. describe here the crystal structure of a native peroxo intermediate of a non-heme diiron enzyme. The 1.7 Å structure reveals a *cis*-μ-1,2 arrangement (*cis*-η^1,η^1-1,2; scheme I of Figure 2A) of the peroxo unit, with a *gauche* Fe-O-O-Fe torsion angle. Remarkably, the O1-atom of the peroxide is more centrally placed between the two iron atoms (2.2 and 2.6 Å from Fe1 and Fe2, respectively), whereas O2 is basically interacting only with Fe2 (3.5 and 2.2 Å from Fe1 and Fe2, respectively) (Figure 2B). While this asymmetric arrangement is still *cis*-μ-1,2 (η^1,η^1-1,2), it is not far from an η^1,η^2-1,2 arrangement (V of Figure 2A), a configuration that has very recently been proposed on the basis of spectroscopic data for the peroxo intermediate of a bacterial aryl oxygenase (Makris et al., 2015). The lack of true isosbestic points in the time-dependent UV/Vis spectra reported by Han et al. (2015) suggests that the peroxo intermediate may adopt a continuum of configurations and this may be reflected in the slight differences observed between the two molecules in the asymmetric unit of the hDOHH crystal.

The crystallographic work of Han et al. also reveals the reason for the unusual stability of the peroxo intermediate of hDOHH: in contrast to all other well-characterized non-heme diiron enzymes, hDOHH features a histidine-rich coordination of the diiron core lacking any bridging carboxylates. The histidines coordinate iron through their Nε-atoms, not

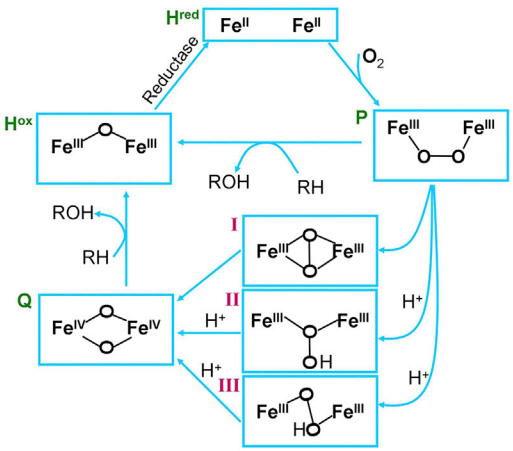

Figure 1. Catalytic Cycle of sMMOH

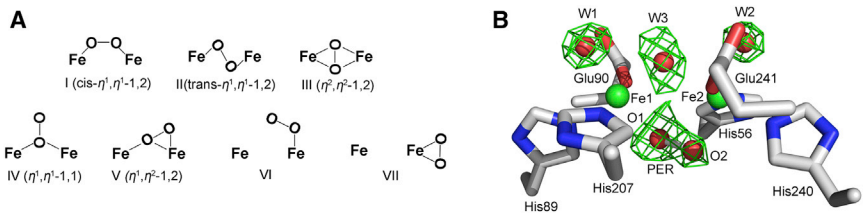

Figure 2. Peroxo-diiron(III) Core

(A) Possible geometries for the peroxo-diiron(III) core of diiron-containing oxygenases; (B) F_o-F_c difference density (contoured at 4.7σ) for the non-protein ligands of the diiron core of hDOHH. The corresponding difference map was calculated after building the protein ligands but before incorporating the peroxo, and water ligands.

their Nδ-atoms as in most other diiron oxygenases. Furthermore, the secondary ligation hemisphere surrounding the binding site for the peroxide ion is very hydrophobic, shielding the reactive intermediate by a methionine pair and a leucine pair. Importantly, potential hydrogen-bonding donors such as threonine, which occur in many O_2-activating monooxygenases, where they seem to shuttle protons to the active site (Wallar and Lipscomb, 1996), are completely absent from the hDOHH active site; therefore, the heterolytic breakdown of the peroxide resulting from protonation is greatly delayed.

A high-oxidation state intermediate such as compound **Q** has so far not been described for hDOHH, and perhaps there is no requirement for it. In the sMMOH system, **Q** is the active species that breaks the unusually strong (ΔH = 105 kcal mol^{-1}) C-H bond in methane to insert oxygen. However, the peroxo-diiron(III) intermediate **P** of sMMOH is by itself able to oxidize electron-rich hydrocarbons such as diethyl ether or propylene (indicated by the direct pathway between **P** and $\mathbf{H^{ox}}$ in Figure 1) (Tinberg and Lippard, 2010).

There is only one substrate known for DOHH: deoxyhypusine eukaryotic translation initiation factor 5A (eIF-5A). The various functions of this protein in translation initiation and elongation (in particular of oligoproline-containing polypeptide segments) and in nuclear export of retroviral RNA, CD83 mRNA, and iNOS mRNA depend on the elongation of an exposed lysine residue (K50 in the human protein) by attachment of a 2-hydroxo-4-amino butyl unit. This unique posttranslational modification is performed in a two-step reaction catalyzed by the enzymes deoxyhypusine synthase (DHS) and DOHH (Park, 2006). In the first step, DHS attaches a 4-aminobutyl group originating from spermidine to the Nζ atom of residue K50, to yield deoxyhypusine-eIF-5A (Dhp-eIF-5A). In the second step, DOHH hydroxylates Dhp-eIF-5A in the 2-position of the 4-aminobutyl group, thereby affording hypusine-eIF-5A (Hpu-eIF-5A). The structures presented by Han et al. (2015) immediately suggest how the substrate and the product would bind to human DOHH. This in itself is a major achievement, as hDOHH could well act as a target for the development of therapeutics for the treatment of HIV/AIDS, certain cancers, and diabetes (Kaiser, 2012).

REFERENCES

Banerjee, R., Proshlyakov, Y., Lipscomb, J.D., and Proshlyakov, D.A. (2015). Nature *518*, 431–434.

Han, Z., Sakai, N., Böttger, L.H., Klinke, S., Hauber, J., Trautwein, A.X., and Hilgenfeld, R. (2015). Structure *23*, this issue, 882–892.

Kaiser, A. (2012). Amino Acids *42*, 679–684.

Liu, K.E., Valentine, A.M., Qiu, D., Edmondson, D.E., Appelman, E.H., Spiro, T.G., and Lippard, S.J. (1995). J. Am. Chem. Soc. *117*, 4997–4998.

Makris, T.M., Vu, V.V., Meier, K.K., Komor, A.J., Rivard, B.S., Münck, E., Que, L., Jr., and Lipscomb, J.D. (2015). J. Am. Chem. Soc. *137*, 1608–1617.

Park, M.H. (2006). J. Biochem. *139*, 161–169.

Solomon, E.I., Brunold, T.C., Davis, M.I., Kemsley, J.N., Lee, S.K., Lehnert, N., Neese, F., Skulan, A.J., Yang, Y.S., and Zhou, J. (2000). Chem. Rev. *100*, 235–350.

Tinberg, C.E., and Lippard, S.J. (2010). Biochemistry *49*, 7902–7912.

Tinberg, C.E., and Lippard, S.J. (2011). Acc. Chem. Res. *44*, 280–288.

Vu, V.V., Emerson, J.P., Martinho, M., Kim, Y.S., Münck, E., Park, M.H., and Que, L., Jr. (2009). Proc. Natl. Acad. Sci. USA *106*, 14814–14819.

Wallar, B.J., and Lipscomb, J.D. (1996). Chem. Rev. *96*, 2625–2658.

Xue, G., Fiedlera, A.T., Martinho, M., Münck, E., and Que, L., Jr. (2008). Proc. Natl. Acad. Sci. USA *105*, 20615–20620.

